AMSI SUMMER RESEARCH SCHOLARSHIPS 2025–26

Get a taste for Research this Summer

The Drug Diffusion Problem: Comparison of Analytic Methods

Noah Cresp

Supervised by Prof. Natalie Thamwattana and Dr. Dave Smith

The University of Newcastle

Jane Street®

AMSI AUSTRALIAN MATHEMATICAL SCIENCES INSTITUTE

Contents

Abstract

We consider a two-layer diffusion problem representing transdermal drug delivery as a one-dimensional model. The model describes Fickian diffusion in each layer, coupled by continuity of flux and a partition condition at the interface, together with appropriate boundary conditions. It is solved analytically using two distinct methods, the Laplace transform approach and the Unified Transform Method (Fokas' Method). We compare the resulting solution representations and discuss practical considerations for computation, including inversion and numerical evaluation. This highlights strengths and weaknesses of each method, especially in the context of extending the model to more layers or modified boundary and interface conditions.

1 Introduction

Percutaneous, or transdermal, drug delivery refers to the transport of a drug from an external source across the skin's outer layers and into deeper tissue, whence it enters systemic circulation. Because the skin is a strong barrier to mass transfer, diffusion through the outer layers is often rate-limiting, and the relevant time scales can range from minutes to days, depending on the drug and formulation. This route of drug application is attractive because it can enable controlled, sustained dosing while avoiding gastrointestinal degradation and first-pass metabolism, and it can reduce the need for repeated injections. Transdermal delivery is also a clinically established technology: there are many approved systems delivering drugs such as estradiol, fentanyl, lidocaine and testosterone, as well as combination patches and device assisted systems used in analgesia. (Prausnitz & Langer, 2008) However, these advantages depend strongly on the underlying transport through the skin, so modelling is useful for predicting uptake and guiding design choices. Even simplified diffusion models can capture essential pharmacokinetic features, such as sustained release and the resulting plasma profiles under controlled dosing conditions. (Guy & Hadgraft, 1985)

A common setup consists of a vehicle, such as a patch, containing a drug in contact with the skin. This can be described mathematically by a multilayer diffusion problem, with one diffusion equation posed in each material layer. In transdermal settings, this approach is widely used to connect measurable parameters to macroscopic transport behaviour (Fernandes et al., 2005). In each region, the concentration evolves by Fick's law. The layers are then coupled by interface conditions which enforce conservation of mass through a continuity of flux condition, together with a partition relationship describing a concentration jump due to different solubilities across the interface. These interfacial effects are very important in composite diffusion models and are also studied more generally in the context of heat diffusion with imperfect contact between adjacent media (Sheils, 2017).

In practice, predicted transport can vary substantially with the diffusion coefficients, the partition coefficient, and the relative thickness of each layer. This makes it useful to have solution methods that behave well across parameter ranges, and that do not require a completely new derivation each time the model is modified. A classical approach is the Laplace transform method. In multilayer settings it often produces explicit transformed solutions, but the inversion step can become algebraically heavy and typically leads to series representations

governed by transcendental eigenvalue conditions (Rodrigo & Worthy, 2016). For more complicated interface or boundary conditions, the inversion can be difficult to carry out in closed form.

An alternative is the Unified Transform Method (UTM), or Fokas Method, which has been used for interface problems and composite media (Sheils, 2017). The method builds global relations that couple boundary and interface data, and then uses complex-analytic contour deformation arguments to obtain integral representations of the solution. One advantage is that changes to boundary or interface conditions can often be absorbed at the level of these global relations, rather than restarting ab initio. Motivated by the need for a fuller and more rigorous comparison, we present implementations of both the Laplace inversion and UTM for a transdermal-style two-layer problem.

In this project we model a two-layer vehicle to skin system governed by Fickian diffusion, with flux continuity and a partition condition at the interface. The governing equations and interface structure are taken from a standard formulation of the transdermal model (Fernandes et al., 2005). We derive analytic solutions firstly using a Laplace transform approach, following Fernandes et al. (2005), and secondly employing the Unified Transform Method, using the composite/interface methodology of Deconinck et al. (2014). We then compare and contrast the two methods in terms of derivation complexity, numerical implementation, and how naturally each approach accommodates model extensions.

The remainder of this report is organised as follows. Section 2 presents the mathematical model together with the boundary and interface conditions. Section 3.1 derives the Laplace transform solution and discusses inversion. Section 3.2 develops the Unified Transform Method solution, and Section 4 compares the two approaches and outlines limitations and possible extensions.

Statement of Authorship

I declare that the work presented in this report is my own, except where due acknowledgement is given. The mathematical modelling, analysis, numerical implementation, and comparison of analytic methods were undertaken by the author under the supervision of Prof. Natalie Thamwattana and Dr. Dave Smith.

2 Mathematical Model

We model drug diffusion in a two-layer composite medium (see Figure 1): a vehicle layer $x \in (-a, 0)$ with diffusivity D_1 and a skin layer $x \in (0, b)$ with diffusivity D_2. Concentrations C_1 and C_2 evolve by Fickian diffusion, so they satisfy the diffusion equation. Initially the vehicle is uniformly loaded and the skin is drug-free. We impose a no-flux condition at the impermeable vehicle boundary $x = -a$ representing no drug loss to the external environment, and a perfect sink at the deep skin boundary $x = b$, representing immediate uptake when the drug comes into contact with the blood circulation. At the interface $x = 0$ we enforce conservation of mass via continuity of flux, and imperfect contact/solubility via a partition condition with coefficient k_m. Accordingly, the governing equations together with the initial, boundary, and interface conditions are given by

$$[\partial_t - D_1\partial_{xx}]\, C_1(x,t) = 0, \qquad (x,t) \in (-a,0)\times(0,T) \tag{1.PDE1}$$

$$[\partial_t - D_2\partial_{xx}]\, C_2(x,t) = 0, \qquad (x,t) \in (0,b)\times(0,T) \tag{1.PDE2}$$

$$C_1(x,0) = C_{1,0}, \qquad x \in [-a,0] \tag{1.IC1}$$

$$C_2(x,0) = 0, \qquad x \in [0,b] \tag{1.IC2}$$

$$\frac{\partial C_1}{\partial x}(-a,t) = 0, \qquad t \in [0,T] \tag{1.BC1}$$

$$C_2(b,t) = 0, \qquad t \in [0,T] \tag{1.BC2}$$

$$D_1\frac{\partial C_1}{\partial x}(0^-,t) = D_2\frac{\partial C_2}{\partial x}(0^+,t), \qquad t \in [0,T] \tag{1.BC3}$$

$$C_1(0,t) = k_m C_2(0,t). \qquad t \in [0,T] \tag{1.BC4}$$

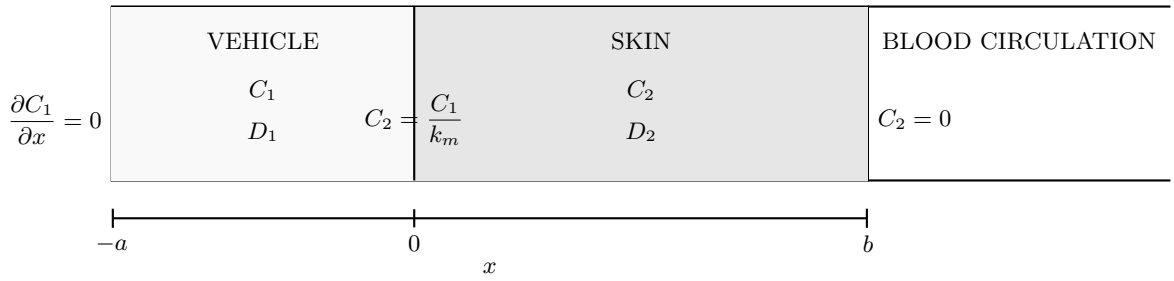

Figure 1: Schematic diagram of two-layer drug diffusion

3 Analytic Methods

3.1 Laplace Transform Method

3.1.1 Laplace transform and transformed ODEs

We take the temporal Laplace transform of (1.PDE1) and (1.PDE2) and apply (1.IC1) and (1.IC2) to obtain:

$$\frac{d^2\bar{C}_1}{dx^2}(x,s) - \frac{s}{D_1}\bar{C}_1(x,s) = -\frac{C_{1,0}}{D_1},$$

and

$$\frac{d^2\bar{C}_2}{dx^2}(x,s) - \frac{s}{D_2}\bar{C}_2(x,s) = 0.$$

These constant-coefficient second-order ODEs have the general solutions

$$\bar{C}_1(x,s) = K_1(s)\cosh\left(\sqrt{\frac{s}{D_1}}(x+a)\right) + \frac{C_{1,0}}{s},$$

$$\bar{C}_2(x,s) = K_2(s)\sinh\left(\sqrt{\frac{s}{D_2}}(b-x)\right).$$

These particular hyperbolic forms are chosen so that the boundary conditions at $x = -a$ and $x = b$ are satisfied identically, namely $\partial_x \bar{C}_1(-a, s) = 0$ and $\bar{C}_2(b, s) = 0$.

Imposing the boundary and interface conditions determines $K_1(s)$ and $K_2(s)$ as

$$K_1(s) = -\frac{C_{1,0}\sqrt{\frac{D_1}{D_2}}\,\cosh\left(\sqrt{\frac{s}{D_2}}\,b\right)}{s\,\Delta(s)},$$

$$K_2(s) = \frac{C_{1,0}}{s\,k_m\,\sinh\left(\sqrt{\frac{s}{D_2}}\,b\right)}\left[1 - \frac{\sqrt{\frac{D_1}{D_2}}\,\cosh\left(\sqrt{\frac{s}{D_2}}\,b\right)\cosh\left(\sqrt{\frac{s}{D_1}}\,a\right)}{\Delta(s)}\right],$$

where

$$\Delta(s) = k_m \sinh\left(\sqrt{\frac{s}{D_2}}\,b\right)\sinh\left(\sqrt{\frac{s}{D_1}}\,a\right) + \sqrt{\frac{D_2}{D_1}}\cosh\left(\sqrt{\frac{s}{D_1}}\,a\right)\cosh\left(\sqrt{\frac{s}{D_2}}\,b\right).$$

3.1.2 Transformed Solutions

Substituting the expressions for $K_1(s)$ and $K_2(s)$ into the general solutions gives the Laplace-domain concentrations

$$\bar{C}_1(x, s) = \frac{C_{1,0}}{s}\left[1 - \frac{\sqrt{\frac{D_2}{D_1}}\,\cosh\left(\sqrt{\frac{s}{D_2}}\,b\right)\cosh\left(\sqrt{\frac{s}{D_1}}(x + a)\right)}{\Delta(s)}\right], \tag{2}$$

and

$$\bar{C}_2(x, s) = \frac{C_{1,0}}{sk_m}\,\frac{\sinh\left(\sqrt{\frac{s}{D_2}}(b - x)\right)}{\sinh\left(\sqrt{\frac{s}{D_2}}\,b\right)}\left[1 - \frac{\sqrt{\frac{D_2}{D_1}}\,\cosh\left(\sqrt{\frac{s}{D_2}}\,b\right)\cosh\left(\sqrt{\frac{s}{D_1}}\,a\right)}{\Delta(s)}\right]. \tag{3}$$

Using the definition of $\Delta(s)$, the bracketed term in (3) satisfies

$$\Delta(s) - \sqrt{\frac{D_2}{D_1}}\cosh\left(\sqrt{\frac{s}{D_2}}\,b\right)\cosh\left(\sqrt{\frac{s}{D_1}}\,a\right) = k_m \sinh\left(\sqrt{\frac{s}{D_2}}\,b\right)\sinh\left(\sqrt{\frac{s}{D_1}}\,a\right),$$

and therefore (3) reduces to

$$\bar{C}_2(x, s) = \frac{C_{1,0}}{s}\,\frac{\sinh\left(\sqrt{\frac{s}{D_2}}(b - x)\right)\sinh\left(\sqrt{\frac{s}{D_1}}\,a\right)}{\Delta(s)}. \tag{4}$$

3.1.3 Inversion

We invert the Laplace-domain solutions using the Bromwich integral and the residue theorem. For C_1, write

$$\bar{C}_1(x, s) = \frac{C_{1,0}}{s} - \frac{C_{1,0}}{s}\,\frac{F_1(x, s)}{\Delta(s)}, \qquad F_1(x, s) := \sqrt{\frac{D_2}{D_1}}\,\cosh\left(b\sqrt{\tfrac{s}{D_2}}\right)\,\cosh\left((x + a)\sqrt{\tfrac{s}{D_1}}\right).$$

Hence

$$\begin{aligned} C_1(x, t) &= \mathcal{L}^{-1}\left\{\frac{C_{1,0}}{s}\right\} - C_{1,0}\,\mathcal{L}^{-1}\left\{\frac{F_1(x, s)}{s\,\Delta(s)}\right\} \\ &= C_{1,0} - C_{1,0}\,\mathcal{L}^{-1}\left\{\frac{F_1(x, s)}{s\,\Delta(s)}\right\} \end{aligned}$$

Hence

$$C_1(x,t) = C_{1,0} - \frac{C_{1,0}}{2\pi i}\int_{\gamma-i\infty}^{\gamma+i\infty} \frac{e^{st}F_1(x,s)}{s\,\Delta(s)}\,ds,$$

where $\gamma > 0$ is chosen so that the contour lies to the right of all singularities. The integrand has simple poles at $s = 0$ and at the simple zeros $\{s_k\}$ of $\Delta(s)$. Closing the contour to the left and applying the residue theorem gives

$$C_1(x,t) = C_{1,0} - C_{1,0}\sum_{s_k:\, s_k\Delta(s_k)=0} \operatorname{Res}\left(\frac{e^{st}F_1(x,s)}{s\,\Delta(s)},\, s = s_k\right).$$

The residue at $s = 0$ cancels the explicit $C_{1,0}$ term, and the remaining contribution is a sum over the zeros of $\Delta(s)$ since $e^{0t}F_1(0) = \Delta(0) = \sqrt{\frac{D_2}{D_1}}$:

$$C_1(x,t) = -C_{1,0}\sum_{s_k:\,\Delta(s_k)=0} \operatorname{Res}\left(\frac{e^{st}F_1(x,s)}{s\,\Delta(s)},\, s = s_k\right).$$

We take $\sqrt{s}$ on the principal branch, with branch cut along $(-\infty, 0]$, and we close the inversion contour so it avoids the cut. Hence the only enclosed singularities are the isolated poles coming from the zeros of $\Delta(s)$. It is convenient to parameterise these poles as

$$s_k = -\lambda_k^2, \qquad \lambda_k > 0,$$

so that $\sqrt{s_k} = i\lambda_k$ on the principal branch, and the hyperbolic factors reduce via $\cosh(i\theta) = \cos\theta$ and $\sinh(i\theta) = i\sin\theta$. Substituting $s = -\lambda^2$ into

$$\Delta(s) = k_m \sinh\left(\sqrt{\frac{s}{D_2}}\,b\right)\sinh\left(\sqrt{\frac{s}{D_1}}\,a\right) + \sqrt{\frac{D_2}{D_1}}\cosh\left(\sqrt{\frac{s}{D_1}}\,a\right)\cosh\left(\sqrt{\frac{s}{D_2}}\,b\right),$$

gives

$$\Delta(-\lambda^2) = -k_m \sin\left(\tfrac{b\lambda}{\sqrt{D_2}}\right)\sin\left(\tfrac{a\lambda}{\sqrt{D_1}}\right) + \sqrt{\frac{D_2}{D_1}}\cos\left(\tfrac{a\lambda}{\sqrt{D_1}}\right)\cos\left(\tfrac{b\lambda}{\sqrt{D_2}}\right).$$

Therefore $\Delta(-\lambda_k^2) = 0$ is equivalent to

$$\tan\left(\tfrac{a}{\sqrt{D_1}}\lambda_k\right)\,\tan\left(\tfrac{b}{\sqrt{D_2}}\lambda_k\right) = \frac{1}{k_m}\sqrt{\frac{D_2}{D_1}}, \tag{5}$$

and, at these poles,

$$F_1(x,-\lambda_k^2) = \sqrt{\frac{D_2}{D_1}}\,\cos\left(\tfrac{b\lambda_k}{\sqrt{D_2}}\right)\,\cos\left(\tfrac{(x+a)\lambda_k}{\sqrt{D_1}}\right).$$

If $\Delta(s_k) = 0$ and $\Delta'(s_k) \neq 0$, then $\frac{1}{\Delta(s)}$ has a simple pole at $s = s_k$ and

$$\operatorname{Res}\left(\frac{g(s)}{\Delta(s)}, s_k\right) = \frac{g(s_k)}{\Delta'(s_k)}.$$

Taking $g(s) = e^{st}F_1(x,s)/s$ yields

$$\operatorname{Res}\left(\frac{e^{st}F_1(x,s)}{s\,\Delta(s)}, s_k\right) = \frac{e^{s_k t}F_1(x,s_k)}{s_k\,\Delta'(s_k)}.$$

For numerical evaluation, we derive $\Delta'(-\lambda_k^2)$ in Appendix A.1.

Therefore we may represent our $C_1(x,t)$ solution as

$$C_1(x,t) = C_{1,0} \sum_{k\geq 1} \left[\frac{\sqrt{\frac{D_2}{D_1}}\,\cos\!\left(\frac{b\lambda_k}{\sqrt{D_2}}\right)}{\lambda_k^2\,\Delta'(-\lambda_k^2)} \right] \cos\!\left(\tfrac{(x+a)\lambda_k}{\sqrt{D_1}}\right) e^{-\lambda_k^2 t}. \tag{6}$$

For C_2 we start from the Laplace-domain representation

$$\bar{C}_2(x,s) = \frac{C_{1,0}}{s}\,\frac{F_2(x,s)}{\Delta(s)}, \qquad F_2(x,s) := \sinh\!\left((b-x)\sqrt{\tfrac{s}{D_2}}\right)\,\sinh\!\left(a\sqrt{\tfrac{s}{D_1}}\right).$$

As before, the inverse transform is evaluated by closing the contour and summing residues at the simple poles $s = s_k$ where $\Delta(s_k) = 0$. The point $s = 0$ does not contribute, since the singularity in $\bar{C}_2(x,s)$ is removable (Appendix A.2). Equivalently, $F_2(x,s) = \mathcal{O}(s)$ as $s \to 0$, so $\bar{C}_2(x,s)$ is bounded at $s = 0$ and has no residue there.

Parameterising the poles by $s_k = -\lambda_k^2$ with $\lambda_k > 0$ and using $\sqrt{s_k} = i\lambda_k$ (principal branch), we obtain

$$F_2(x,-\lambda_k^2) = \sinh\!\left(i\tfrac{(b-x)\lambda_k}{\sqrt{D_2}}\right)\,\sinh\!\left(i\tfrac{a\lambda_k}{\sqrt{D_1}}\right) = -\sin\!\left(\tfrac{(b-x)\lambda_k}{\sqrt{D_2}}\right)\,\sin\!\left(\tfrac{a\lambda_k}{\sqrt{D_1}}\right).$$

Therefore the residue calculation gives

$$C_2(x,t) = C_{1,0} \sum_{k\geq 1} \left[\frac{\sin\!\left(\frac{a\lambda_k}{\sqrt{D_1}}\right)}{\lambda_k^2\,\Delta'(-\lambda_k^2)} \right] \sin\!\left(\tfrac{(b-x)\lambda_k}{\sqrt{D_2}}\right) e^{-\lambda_k^2 t}, \tag{7}$$

where $\{\lambda_k\}_{k\geq 1}$ are the positive solutions of (5).

3.2 Unified Transform Method

3.2.1 Problem reformulation and global relations

We introduce

$$p(x,t) := C_1(-x,t), \qquad 0 < x < a, \qquad q(x,t) := C_2(x,t), \qquad 0 < x < b,$$

so that both concentration functions are posed on positive intervals. The problem becomes

$$[\partial_t - D_1\partial_{xx}]\,p(x,t) = 0, \qquad (x,t) \in (0,a)\times(0,T) \tag{8.PDE1}$$

$$[\partial_t - D_2\partial_{xx}]\,q(x,t) = 0, \qquad (x,t) \in (0,b)\times(0,T) \tag{8.PDE2}$$

$$p(x,0) = C_{1,0}, \qquad x \in [0,a] \tag{8.IC1}$$

$$q(x,0) = 0, \qquad x \in [0,b] \tag{8.IC2}$$

$$\frac{\partial p}{\partial x}(a,t) = 0, \qquad t \in [0,T] \tag{8.BC1}$$

$$q(b,t) = 0, \qquad t \in [0,T] \tag{8.BC2}$$

$$-D_1\frac{\partial p}{\partial x}(0,t) = D_2\frac{\partial q}{\partial x}(0,t), \qquad t \in [0,T] \tag{8.BC3}$$

$$p(0,t) = k_m q(0,t). \qquad t \in [0,T] \tag{8.BC4}$$

Now we define the Fourier Transforms

$$\hat{p}(\lambda,t) := \int_0^a e^{-i\lambda x} p(x,t)\,dx, \qquad \hat{q}(\lambda,t) := \int_0^b e^{-i\lambda x} q(x,t)\,dx.$$

These agree with the usual exponential Fourier Tranforms of p, q, after their extension by zero to the full line. Applying these transforms to (8.PDE1)–(8.PDE2) and integrating by parts twice yields the global relations

$$\hat{p}(\lambda,t)e^{D_1\lambda^2 t} = \hat{p}(\lambda,0) + D_1\int_0^t e^{D_1\lambda^2 s}\Big[i\lambda e^{-i\lambda a}p(a,s) - p_x(0,s) - i\lambda p(0,s)\Big]\,ds, \tag{9.GR: p}$$

$$\hat{q}(\lambda,t)e^{D_2\lambda^2 t} = \hat{q}(\lambda,0) + D_2\int_0^t e^{D_2\lambda^2 s}\Big[e^{-i\lambda b}q_x(b,s) - q_x(0,s) - i\lambda q(0,s)\Big]\,ds. \tag{9.GR: q}$$

The initial data give

$$\hat{p}(\lambda,0) = \int_0^a e^{-i\lambda x}C_{1,0}\,dx = \frac{C_{1,0}}{i\lambda}\big(1-e^{-i\lambda a}\big) =: \hat{P}(\lambda), \qquad \hat{q}(\lambda,0) = 0.$$

Derivations of (9.GR: p)–(9.GR: q) are included in Appendix B.

3.2.2 Ehrenpreis form and spectral boundary data

For $0 \le t \le T$, we define the time-t spectral boundary transforms as

$$f_j^\flat(\lambda;t) := \int_0^t e^{D_1\lambda^2 s}\,\partial_x^j p(0,s)\,ds, \qquad g_j^\flat(\lambda;t) := \int_0^t e^{D_1\lambda^2 s}\,\partial_x^j p(a,s)\,ds,$$

$$f_j^\#(\lambda;t) := \int_0^t e^{D_2\lambda^2 s}\,\partial_x^j q(0,s)\,ds, \qquad g_j^\#(\lambda;t) := \int_0^t e^{D_2\lambda^2 s}\,\partial_x^j q(b,s)\,ds.$$

When convenient we also write $f_j^\flat(\lambda) := f_j^\flat(\lambda;T)$ and similarly for $g_j^\flat, f_j^\#, g_j^\#$, corresponding to the fixed terminal time $T > 0$.

Applying the inverse Fourier transform to the global relations (9.GR: p)–(9.GR: q) yields the preliminary integral representations

$$\begin{aligned} 2\pi p(x,t) = {} & \int_{-\infty}^{\infty} e^{i\lambda x - D_1\lambda^2 t}\,\hat{P}(\lambda)\,d\lambda + D_1\int_{-\infty}^{\infty} e^{i\lambda(x-a)-D_1\lambda^2 t}\left[i\lambda\, g_0^\flat(\lambda;t)\right]d\lambda \\ & - D_1\int_{-\infty}^{\infty} e^{i\lambda x - D_1\lambda^2 t}\left[f_1^\flat(\lambda;t) + i\lambda f_0^\flat(\lambda;t)\right]d\lambda, \end{aligned} \tag{10.P.1}$$

$$2\pi q(x,t) = D_2\int_{-\infty}^{\infty} e^{i\lambda(x-b)-D_2\lambda^2 t}\,g_1^\#(\lambda;t)\,d\lambda - D_2\int_{-\infty}^{\infty} e^{i\lambda x - D_2\lambda^2 t}\left[f_1^\#(\lambda;t) + i\lambda f_0^\#(\lambda;t)\right]d\lambda. \tag{10.P.2}$$

Finally, for later contour deformations we replace the upper limit t by the fixed terminal time T in the spectral boundary transforms. The additional contributions integrate to zero after contour deformation, by analyticity of the transforms and Jordan-type decay estimates (see Appendix B.3). Thus, in the subsequent Ehrenpreis forms we may use $f_j^\flat(\lambda)$, $g_j^\flat(\lambda)$, $f_j^\#(\lambda)$ and $g_j^\#(\lambda)$ (with upper limit T) without changing the resulting solution formulas.

Now we define the following complex regions:

$$\begin{aligned}\mathcal{D}^{\pm} &:= \{\lambda \in \mathbb{C}^{\pm} : \Re(\lambda^2) < 0\} \\ &= \{\lambda = re^{i\theta} : \theta \in \pm(\tfrac{\pi}{4}, \tfrac{3\pi}{4})\},\end{aligned}$$

$$\begin{aligned}\mathcal{E}^{\pm} &:= \{\lambda \in \mathbb{C}^{\pm} : \Re(\lambda^2) > 0\} \\ &= \{\lambda = re^{i\theta} : \theta \in \pm(0, \tfrac{\pi}{4}) \cup \pm(\tfrac{3\pi}{4}, \pi)\}.\end{aligned}$$

And let $\partial\mathcal{D}^{\pm}$ and $\partial\mathcal{E}^{\pm}$ denote the positively oriented boundaries of $\mathcal{D}^{\pm}$ and $\mathcal{E}^{\pm}$, respectively, as shown in Figure 2.

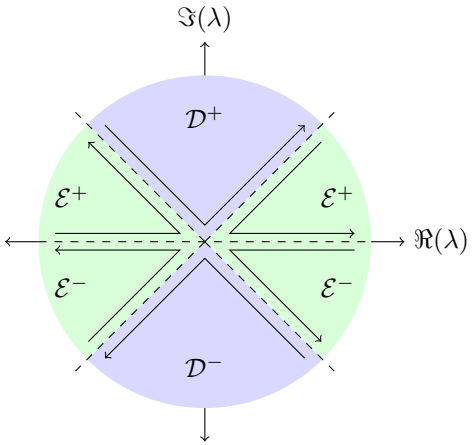

Figure 2: Regions $\mathcal{D}^{\pm}$ and $\mathcal{E}^{\pm}$ in the λ-plane.

Lemma 0.1.

$$\int_{\partial\mathcal{E}^+} e^{i\lambda x - D_1\lambda^2 t}\left[f_1^\flat(\lambda) + i\lambda f_0^\flat(\lambda)\right] d\lambda = 0, \tag{L0.1a}$$

$$\int_{\partial\mathcal{E}^-} e^{i\lambda(x-a) - D_1\lambda^2 t}\left[i\lambda g_0^\flat(\lambda)\right] d\lambda = 0. \tag{L0.1b}$$

Proof: See Appendix B.4.

So we redefine the integral boundaries of (10.P.1).

$$\begin{aligned}\Rightarrow \quad 2\pi p(x,t) = &\int_{-\infty}^{\infty} e^{i\lambda x - D_1\lambda^2 t}\,\hat{P}(\lambda)\,d\lambda - D_1\left\{\int_{\partial\mathcal{D}^-} + \int_{\partial\mathcal{E}^-}\right\} e^{i\lambda(x-a) - D_1\lambda^2 t}\left[i\lambda g_0^\flat(\lambda)\right] d\lambda \\ &- D_1\left\{\int_{\partial\mathcal{D}^+} + \int_{\partial\mathcal{E}^+}\right\} e^{i\lambda x - D_1\lambda^2 t}\left[f_1^\flat(\lambda) + i\lambda f_0^\flat(\lambda)\right] d\lambda.\end{aligned}$$

Applying (L0.1b) to the second integral and (L0.1a) to the third, we obtain

$$\begin{aligned}2\pi p(x,t) = &\int_{-\infty}^{\infty} e^{i\lambda x - D_1\lambda^2 t}\,\hat{P}(\lambda)\,d\lambda - D_1\int_{\partial\mathcal{D}^-} e^{i\lambda(x-a) - D_1\lambda^2 t}\left[i\lambda g_0^\flat(\lambda)\right] d\lambda \\ &- D_1\int_{\partial\mathcal{D}^+} e^{i\lambda x - D_1\lambda^2 t}\left[f_1^\flat(\lambda) + i\lambda f_0^\flat(\lambda)\right] d\lambda.\end{aligned} \tag{11.EF: p}$$

We similarly apply contour vanishing arguments analogous to Lemma 0.1 to (10.P.2) to obtain

$$2\pi q(x,t) = -D_2\int_{\partial\mathcal{D}^-} e^{i\lambda(x-b) - D_2\lambda^2 t}\,g_1^\#(\lambda)\,d\lambda - D_2\int_{\partial\mathcal{D}^+} e^{i\lambda x - D_2\lambda^2 t}\left[f_1^\#(\lambda) + i\lambda f_0^\#(\lambda)\right] d\lambda. \tag{11.EF: q}$$

These are our Ehrenpreis forms for p and q. However, these representations depend on the six unknowns $g_0^\flat(\lambda)$, $f_1^\flat(\lambda)$, $f_0^\flat(\lambda)$, $g_1^\#(\lambda)$, $f_1^\#(\lambda)$, and $f_0^\#(\lambda)$. These are related by the global relations evaluated at $t = T$ together with the interface conditions.

3.2.3 Scaled system and elimination of unknown spectral data

In the global relations (9.GR: p)–(9.GR: q) the time exponentials have the form $e^{D_j\lambda^2 s}$. To work with a single phase $e^{\lambda^2 s}$ across both layers, we reparameterise the spectral variable by

$$\lambda \mapsto \frac{\lambda}{\sqrt{D_j}} \qquad (j = 1, 2),$$

so that $D_j(\lambda/\sqrt{D_j})^2 = \lambda^2$. (We will also use $\lambda \mapsto -\lambda/\sqrt{D_j}$ later.)

Previously we defined

$$f_j^\flat(\lambda) := \int_0^T e^{D_1\lambda^2 s}\,\partial_x^j p(0,s)\,ds, \qquad g_j^\flat(\lambda) := \int_0^T e^{D_1\lambda^2 s}\,\partial_x^j p(a,s)\,ds,$$

$$f_j^\#(\lambda) := \int_0^T e^{D_2\lambda^2 s}\,\partial_x^j q(0,s)\,ds, \qquad g_j^\#(\lambda) := \int_0^T e^{D_2\lambda^2 s}\,\partial_x^j q(b,s)\,ds.$$

Under the reparameterisation above, it is natural to introduce the rescaled quantities

$$F_j^\flat(\lambda) := \int_0^T e^{\lambda^2 s}\,\partial_x^j p(0,s)\,ds, \qquad G_j^\flat(\lambda) := \int_0^T e^{\lambda^2 s}\,\partial_x^j p(a,s)\,ds,$$

$$F_j^\#(\lambda) := \int_0^T e^{\lambda^2 s}\,\partial_x^j q(0,s)\,ds, \qquad G_j^\#(\lambda) := \int_0^T e^{\lambda^2 s}\,\partial_x^j q(b,s)\,ds.$$

Then, by direct substitution of $\lambda/\sqrt{D_j}$ into the original definitions,

$$f_j^\flat\left(\frac{\lambda}{\sqrt{D_1}}\right) = F_j^\flat(\lambda), \qquad g_j^\flat\left(\frac{\lambda}{\sqrt{D_1}}\right) = G_j^\flat(\lambda), \qquad f_j^\#\left(\frac{\lambda}{\sqrt{D_2}}\right) = F_j^\#(\lambda), \qquad g_j^\#\left(\frac{\lambda}{\sqrt{D_2}}\right) = G_j^\#(\lambda).$$

Even symmetry. Each of $F_j^\flat, G_j^\flat, F_j^\#, G_j^\#$ depends on λ only through λ^2, hence

$$F_j^\flat(-\lambda) = F_j^\flat(\lambda), \quad G_j^\flat(-\lambda) = G_j^\flat(\lambda), \quad F_j^\#(-\lambda) = F_j^\#(\lambda), \quad G_j^\#(-\lambda) = G_j^\#(\lambda).$$

This $\lambda \mapsto -\lambda$ symmetry will be used when combining transformed relations to eliminate unknown spectral boundary terms.

So now, to relate these unknown boundary values, we start with the global relation for p evaluated at $t = T$,

$$\hat{p}(\lambda;T)e^{D_1\lambda^2 T} = \hat{P}(\lambda) + D_1\Big[i\lambda e^{-i\lambda a}\,g_0^\flat(\lambda) - f_1^\flat(\lambda) - i\lambda f_0^\flat(\lambda)\Big]. \tag{12}$$

We apply the changes of variables $\lambda \to \pm\lambda/\sqrt{D_1}$ and apply the new scaled spectral functions. This gives

$$\hat{p}\left(\frac{\lambda}{\sqrt{D_1}};T\right)e^{\lambda^2 T} = \hat{P}\left(\frac{\lambda}{\sqrt{D_1}}\right) + i\sqrt{D_1}\,\lambda\,e^{-i\lambda a/\sqrt{D_1}}\,G_0^\flat(\lambda) - D_1F_1^\flat(\lambda) - i\sqrt{D_1}\,\lambda\,F_0^\flat(\lambda), \tag{13}$$

$$\hat{p}\left(-\frac{\lambda}{\sqrt{D_1}};T\right)e^{\lambda^2 T} = \hat{P}\left(-\frac{\lambda}{\sqrt{D_1}}\right) - i\sqrt{D_1}\,\lambda\,e^{\,i\lambda a/\sqrt{D_1}}\,G_0^\flat(\lambda) - D_1F_1^\flat(\lambda) + i\sqrt{D_1}\,\lambda\,F_0^\flat(\lambda). \tag{14}$$

Scaled global relations for q

The global relation for q at $t = T$ is written as

$$\hat{q}(\lambda;T)e^{D_2\lambda^2 T} = D_2\Big[e^{-i\lambda b}\,g_1^\#(\lambda) - f_1^\#(\lambda) - i\lambda f_0^\#(\lambda)\Big],$$

then applying $\lambda \to \pm\lambda/\sqrt{D_2}$ and using the new spectral functions gives the scaled pair

$$\hat{q}\left(\frac{\lambda}{\sqrt{D_2}};T\right)e^{\lambda^2 T} = D_2\Big[e^{-i\lambda b/\sqrt{D_2}}\,G_1^\#(\lambda) - F_1^\#(\lambda) - i\frac{\lambda}{\sqrt{D_2}}\,F_0^\#(\lambda)\Big], \tag{15}$$

$$\hat{q}\left(-\frac{\lambda}{\sqrt{D_2}};T\right)e^{\lambda^2 T} = D_2\Big[e^{\,i\lambda b/\sqrt{D_2}}\,G_1^\#(\lambda) - F_1^\#(\lambda) + i\frac{\lambda}{\sqrt{D_2}}\,F_0^\#(\lambda)\Big]. \tag{16}$$

Now we can consider (8.BC3) and (8.BC4).

From (8.BC3), we have $p_x(0,t) = -\frac{D_2}{D_1} q_x(0,t)$

$$\Rightarrow e^{\lambda^2 t} p_x(0,t) = -\frac{D_2}{D_1} e^{\lambda^2 t} q_x(0,t)$$
$$\Rightarrow \int_0^T e^{\lambda^2 s} p_x(0,s)ds = -\frac{D_2}{D_1} \int_0^T e^{\lambda^2 s} q_x(0,s)ds$$
$$\Rightarrow F_1^\flat(\lambda) = -\frac{D_2}{D_1} F_1^\#(\lambda).$$

In (8.BC4), we have $p(0,t) = k_m q(0,t)$, we do the same process:

$$\Rightarrow F_0^\flat(\lambda) = k_m\, F_0^\#(\lambda)$$

We apply these BCs to equations (13) and (14) to obtain:

$$\hat{p}\left(\frac{\lambda}{\sqrt{D_1}}; T\right) e^{\lambda^2 T} = \hat{P}\left(\frac{\lambda}{\sqrt{D_1}}\right) + i\sqrt{D_1}\,\lambda\, e^{-i\lambda a/\sqrt{D_1}}\, G_0^\flat(\lambda) + D_2 F_1^\#(\lambda) - i\sqrt{D_1}\,\lambda\, k_m\, F_0^\#(\lambda), \tag{17}$$

$$\hat{p}\left(-\frac{\lambda}{\sqrt{D_1}}; T\right) e^{\lambda^2 T} = \hat{P}\left(-\frac{\lambda}{\sqrt{D_1}}\right) - i\sqrt{D_1}\,\lambda\, e^{i\lambda a/\sqrt{D_1}}\, G_0^\flat(\lambda) + D_2 F_1^\#(\lambda) + i\sqrt{D_1}\,\lambda\, k_m\, F_0^\#(\lambda). \tag{18}$$

Now we have a system of four equations (15) - (18) relating four unknowns. In matrix form, we have

$$\begin{pmatrix} i\sqrt{D_1}\,\lambda e^{\frac{-i\lambda a}{\sqrt{D_1}}} & 0 & -i\sqrt{D_1}\,k_m\lambda & D_2 \\ -i\sqrt{D_1}\,\lambda e^{\frac{i\lambda a}{\sqrt{D_1}}} & 0 & i\sqrt{D_1}\,k_m\lambda & D_2 \\ 0 & D_2 e^{\frac{-i\lambda b}{\sqrt{D_2}}} & -i\lambda\sqrt{D_2} & -D_2 \\ 0 & D_2 e^{\frac{i\lambda b}{\sqrt{D_2}}} & i\lambda\sqrt{D_2} & -D_2 \end{pmatrix} \begin{pmatrix} G_0^\flat(\lambda) \\ G_1^\#(\lambda) \\ F_0^\#(\lambda) \\ F_1^\#(\lambda) \end{pmatrix} = e^{\lambda^2 T} \begin{pmatrix} \hat{p}\left(\frac{\lambda}{\sqrt{D_1}}; T\right) \\ \hat{p}\left(-\frac{\lambda}{\sqrt{D_1}}; T\right) \\ \hat{q}\left(\frac{\lambda}{\sqrt{D_2}}; T\right) \\ \hat{q}\left(-\frac{\lambda}{\sqrt{D_2}}; T\right) \end{pmatrix} - \begin{pmatrix} \hat{P}\left(\frac{\lambda}{\sqrt{D_1}}\right) \\ \hat{P}\left(-\frac{\lambda}{\sqrt{D_1}}\right) \\ 0 \\ 0 \end{pmatrix}.$$

A full derivation of the solution to this system can be found at Appendix B.5

Substitution into the Ehrenpreis forms

Starting from (11.EF: p), we use the rescalings defined previously,

$$g_0^\flat(\lambda) = G_0^\flat(\lambda\sqrt{D_1}), \qquad f_1^\flat(\lambda) = -\frac{D_2}{D_1} F_1^\#(\lambda\sqrt{D_1}), \qquad f_0^\flat(\lambda) = k_m F_0^\#(\lambda\sqrt{D_1}),$$

and a redefinition of our spectral parameters based on decay on complex contours, to obtain

$$\begin{aligned} 2\pi p(x,t) = &\int_{-\infty}^{\infty} e^{i\lambda x - D_1\lambda^2 t}\, \hat{P}(\lambda)\, d\lambda - D_1 \int_{\partial\mathcal{D}^-} e^{i\lambda(x-a) - D_1\lambda^2 t} \left[i\lambda\, \widetilde{G}_0^\flat(\lambda\sqrt{D_1})\right] d\lambda \\ &- D_1 \int_{\partial\mathcal{D}^+} e^{i\lambda x - D_1\lambda^2 t} \left[-\frac{D_2}{D_1} \widetilde{F}_1^\#(\lambda\sqrt{D_1}) + i\lambda k_m \widetilde{F}_0^\#(\lambda\sqrt{D_1})\right] d\lambda. \end{aligned} \tag{19}$$

Likewise, for $q(x,t)$,

$$2\pi q(x,t) = -D_2 \int_{\partial\mathcal{D}^-} e^{i\lambda(x-b) - D_2\lambda^2 t}\, \widetilde{G}_1^\#(\lambda\sqrt{D_2})\, d\lambda - D_2 \int_{\partial\mathcal{D}^+} e^{i\lambda x - D_2\lambda^2 t} \left[\widetilde{F}_1^\#(\lambda\sqrt{D_2}) + i\lambda \widetilde{F}_0^\#(\lambda\sqrt{D_2})\right] d\lambda. \tag{20}$$

Here $\widetilde{G}_0^{\flat}, \widetilde{G}_1^{\#}, \widetilde{F}_0^{\#}, \widetilde{F}_1^{\#}$ denote the corresponding spectral terms with the exponentially decaying contributions (on $\partial\mathcal{D}^{\pm}$) removed, and are as follows:

$$\widetilde{G}_0^{\flat}(\lambda) = \frac{\widetilde{R}_1 k_m \sqrt{D_2}\sin\left(\frac{b\lambda}{\sqrt{D_2}}\right) - \widetilde{R}_2 D_2 \cos\left(\frac{b\lambda}{\sqrt{D_2}}\right)}{\Delta(\lambda)}, \quad \widetilde{G}_1^{\#}(\lambda) = \frac{\lambda\left(\widetilde{R}_2\sqrt{D_1}\sin\left(\frac{a\lambda}{\sqrt{D_1}}\right) - \widetilde{R}_1\cos\left(\frac{a\lambda}{\sqrt{D_1}}\right)\right)}{\Delta(\lambda)},$$

$$\widetilde{F}_0^{\#}(\lambda) = -\frac{\sqrt{D_2}}{\lambda}\sin\left(\frac{b\lambda}{\sqrt{D_2}}\right)\widetilde{G}_1^{\#}(\lambda), \qquad \widetilde{F}_1^{\#}(\lambda) = \cos\left(\frac{b\lambda}{\sqrt{D_2}}\right)\widetilde{G}_1^{\#}(\lambda),$$

and

$$\widetilde{R}_1 = -\frac{1}{2}\left[\hat{P}\left(\frac{\lambda}{\sqrt{D_1}}\right) + \hat{P}\left(-\frac{\lambda}{\sqrt{D_1}}\right)\right], \qquad \widetilde{R}_2 = -\frac{1}{2i\sqrt{D_1}}\left[\hat{P}\left(\frac{\lambda}{\sqrt{D_1}}\right) - \hat{P}\left(-\frac{\lambda}{\sqrt{D_1}}\right)\right].$$

4 Discussion and Comparisons

4.1 Consistency of the two representations

Both the Laplace and UTM approaches solve the same diffusion model (1). The Laplace method produces series representations (6)–(7) obtained by residue inversion at the poles $s_k = -\lambda_k^2$, where the λ_k satisfy the transcendental condition (5). The UTM instead yields contour integral representations (19)–(20) after elimination of unknown spectral boundary data via the scaled global relations. As shown in Figure 3, the numerical evaluation of these two representations produces indistinguishable concentration profiles over the spatial domains and times considered.

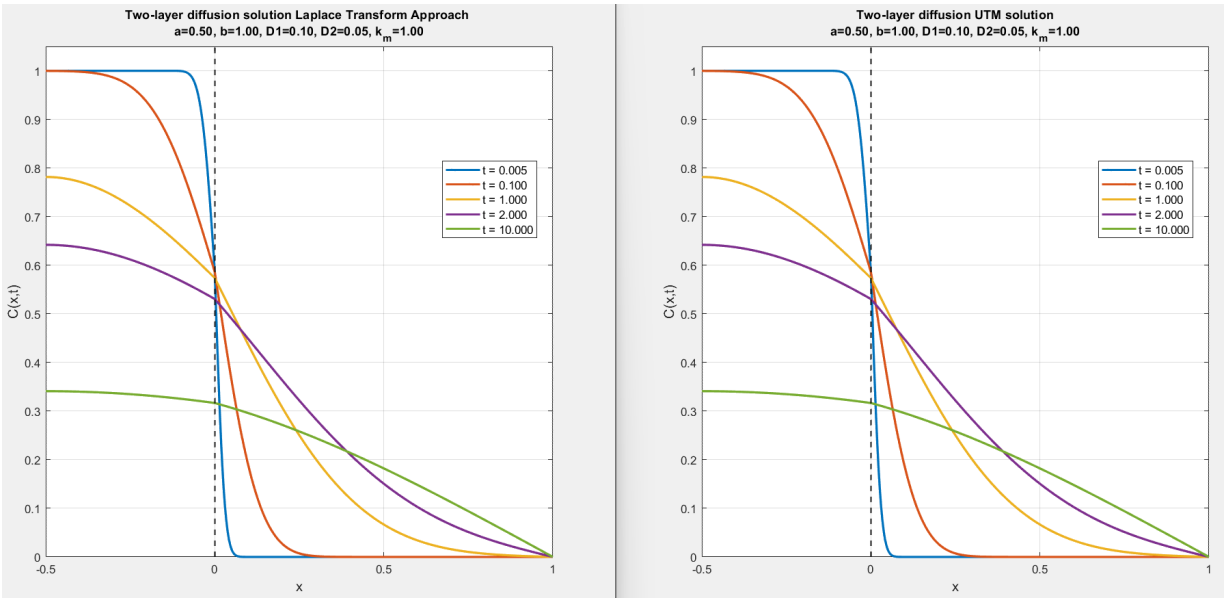

(a) Laplace transform series solution profiles

(b) UTM contour solution profiles

Figure 3: Concentration profiles obtained from the (a) Laplace transform series and (b) UTM contour representations.

The parameters used to generate Fig. 3 were chosen as a representative test case to illustrate consistency of the two approaches. This agreement provides a validation check on both derivations, in particular the handling of the interface conditions and the implementation of the numerical inversion.

4.2 Laplace transform method: strengths and limitations

A practical advantage of the Laplace transform approach is that it reduces the PDE system to constant-coefficient ODEs in x, producing compact transformed solutions (2) and (4). The physical structure of the model is visible already in the Laplace domain: boundary conditions are enforced by the choice of hyperbolic basis functions, while the interface coupling appears through the single denominator $\Delta(s)$. In particular, the poles of $\frac{1}{\Delta(s)}$ encode the relaxation time scales of the composite system, and the resulting inversion naturally leads to a modal decomposition with decay rates $e^{-\lambda_k^2 t}$.

However, the main cost of this method is the inversion step. Even in the two-layer setting, inversion requires a careful analytic description of the singularities, together with explicit residue calculations at the zeroes of $\Delta(s)$. The eigenvalues λ_k are not available in closed form, but must be obtained numerically from (5). This makes the numerical implementation a coupled task. One must compute a sufficiently large set of roots $\{\lambda_k\}$, and then evaluate the weights involving $\Delta'(-\lambda_k^2)$, and finally choose a truncation level K so that the remaining tail is negligible for the times of interest.

The convergence behaviour is strongly time-dependent. For large t, the exponential factors $e^{-\lambda_k^2 t}$ give rapid decay, and relatively few terms are needed. But for small t, many modes contribute, so the truncated series may converge slowly unless K is taken large. This is typical for eigenfunction expansions of diffusion problems and is not specific to this model, but it becomes more pronounced as the geometry becomes thinner with small a or b or the diffusivities D_j are large, since the characteristic decay times shorten. In multilayer extensions, the algebraic complexity of $\Delta(s)$ grows and the eigenvalue problem typically becomes more complicated, so the analytic inversion and residue bookkeeping can become arduous or near-impossible, making a numerical inversion approach an enticing route.

4.3 Unified Transform Method: strengths and limitations

The UTM reorganises the same problem around global relations (9.GR: p) and (9.GR: q), which couple transforms of the solution to spectral boundary data. A key structural difference is that the method treats boundary and interface conditions at the level of these global relations, rather than embedding them through an eigenfunction expansion route. After contour deformation, the Ehrenpreis forms (11.EF: p) and (11.EF: q) express the solution in terms of integrals over $\partial\mathcal{D}^{\pm}$, and unknown spectral boundary values are eliminated by solving the scaled linear system (15)–(18).

One practical advantage is that changing the initial conditions modifies only the initial transform $\hat{P}(\lambda)$ (and $\hat{Q}(\lambda)$ if nonzero inital data is prescribed in the skin layer), while changes to boundary or interface conditions typically alter only the linear algebraic system relating the spectral boundary values, leaving the overall contour

representation intact. This is especially attractive for composite and multilayer media, where the interface conditions can be incorporated systematically into a spectral system that is larger but still linear. In that sense, the UTM is well-suited for extending the present model to more layers or alternative coupling laws.

But the main drawback is its technical complexity. Derivation requires analyticity and decay arguments (for example Lemma 0.1 and the replacement of t by T in the spectral transforms), careful contour definitions, and a nontrivial elimination step. From a computational perspective, the method replaces root-finding and series truncation by numerical contour integration of oscillatory integrals. Accurate quadrature can require attention to parametrisation of $\partial\mathcal{D}^{\pm}$, handling of cancellation, and a sufficiently large contour radius to capture the main contribution while retaining decay from $e^{-D_j\lambda^2 t}$. In practice, the UTM can be computationally heavier, although it avoids the need to compute many eigenvalues, and it behaves well for small t where series methods may require many terms.

4.4 Comparison between two approaches

For the two-layer problem studied here, both methods produce usable analytic representations and agree numerically. Their differences are primarily in (i) the location of difficulty and (ii) how naturally they generalise.

Derivation effort. The Laplace transform method is direct and straightforward up to the transformed solutions (2)–(4), but inversion requires residue analysis tied to $\Delta(s)$ and its zeros. The UTM requires more complex analysis through global relations, contour deformation and analyticity arguments, but once established it yields a systematic route to incorporate boundary and interface information.

Numerical evaluation. Laplace inversion yields rapidly convergent series for moderate t, but may require many terms for small t and depends on stable computation of the eigenvalues and weights. The UTM avoids eigenvalue computation but requires contour quadrature of oscillatory integrals, which can be more expensive per evaluation. In many parameter regimes, the Laplace series is efficient once roots are available, while the UTM is robust across changes in problem data and is less sensitive to the need for very large truncation at early times.

Extensibility. For additional layers, modified boundary conditions, or more complicated interface setups, the Laplace transform approach can become algebraically demanding, as $\Delta(s)$ becomes more complex and the inversion step may not admit a clean residue structure. The UTM tends to scale more naturally: additional layers enlarge the spectral system but preserve the same overall contour-deformation framework. This supports the use of the UTM as a flexible analytic tool for composite diffusion models beyond the basic two-layer setting.

5 Future Work

There are several natural extensions of the present model and methodology.

1. *More realistic distal boundary conditions.* Replacing the perfect sink $C_2(b,t) = 0$ by a Robin condition $D_2C_{2,x}(b,t) = h\,C_2(b,t)$ would model finite uptake into blood and is common in transport modelling. This

modification is straightforward within the UTM framework (altering the spectral system), and it would be useful to compare the resulting Laplace inversion complexity with the two-layer case.

2. *Multilayer skin structure.* Adding a stratum corneum, viable epidermis, and dermis layer leads to a genuine multilayer composite medium with multiple partitions and flux matching conditions. A direct comparison of how $\Delta(s)$ and its eigenvalue condition scale versus how the UTM spectral system scales would sharpen the practical conclusions of this report.

3. *Time-dependent and nonlinear interface laws.* In practice, the interface condition at $x = 0$ may vary in time due to hydration, temperature, occlusion, or changes in formulation, so it is natural to consider a time-dependent partition coefficient $k_m(t)$, or more general interface laws that include an interfacial resistance like imperfect contact, or nonlinear sorption. These modifications affect the coupling conditions and therefore have a large impact on predicted uptake. A useful direction would be to examine how each analytic framework adapts when k_m is replaced by $k_m(t)$, or when the interface condition is replaced by a resistance-type law coupling flux to a concentration jump.

4. *Reaction, binding, or clearance in skin.* Including a linear reaction term in the skin layer, or reversible binding, leads to a reaction-diffusion PDE that can represent metabolism or binding kinetics. Both Laplace transform and UTM methods can still apply in linear settings, but the balance between Laplace inversion complexity and the contour based elimination in the UTM must be reassessed, since the reaction term changes the analytic structure of the transforms.

5. *Parameter estimation and sensitivity.* Given experimental concentration-time data or flux measurements, one could study identifiability and sensitivity with respect to (D_1, D_2, k_m, a, b). This would connect the analytic representations to practical inference problems and clarify which parameters are most influential in different time regimes.

Acknowledgements

I would like to thank the Australian Mathematical Sciences Institute (AMSI) and Jane Street for funding this research and for the opportunity to connect with like-minded people and discover interesting research through AMSIConnect. I would also like to thank my supervisors, Prof. Natalie Thamwattana and Dr. Dave Smith, for their time and support in making this project possible, especially over the holiday period. Finally, I would like to thank Dr. Ravi Pethiyagoda for help with troubleshooting code.

A Laplace Transform Derivations

A.1 Derivative of $\Delta(s)$ at the poles

Recall

$$\Delta(s) = k_m \sinh\Big(b\sqrt{\tfrac{s}{D_2}}\Big)\sinh\Big(a\sqrt{\tfrac{s}{D_1}}\Big) + \sqrt{\frac{D_2}{D_1}}\cosh\Big(a\sqrt{\tfrac{s}{D_1}}\Big)\cosh\Big(b\sqrt{\tfrac{s}{D_2}}\Big).$$

Differentiating and evaluating at $s = s_k$ gives

$$\Delta'(s_k) = k_m\left[\frac{b}{2\sqrt{D_2\, s_k}}\cosh\Big(b\sqrt{\tfrac{s_k}{D_2}}\Big)\sinh\Big(a\sqrt{\tfrac{s_k}{D_1}}\Big) + \sinh\Big(b\sqrt{\tfrac{s_k}{D_2}}\Big)\frac{a}{2\sqrt{D_1\, s_k}}\cosh\Big(a\sqrt{\tfrac{s_k}{D_1}}\Big)\right]$$
$$+\sqrt{\frac{D_2}{D_1}}\left[\frac{a}{2\sqrt{D_1\, s_k}}\sinh\Big(a\sqrt{\tfrac{s_k}{D_1}}\Big)\cosh\Big(b\sqrt{\tfrac{s_k}{D_2}}\Big) + \cosh\Big(a\sqrt{\tfrac{s_k}{D_1}}\Big)\frac{b}{2\sqrt{D_2\, s_k}}\sinh\Big(b\sqrt{\tfrac{s_k}{D_2}}\Big)\right].$$

Setting $s_k = -\lambda_k^2$ with $\lambda_k > 0$ so that $\sqrt{s_k} = i\lambda_k$ on the principal branch gives rise to

$$\Delta'(-\lambda_k^2) = k_m\left[\frac{b}{2\lambda_k\sqrt{D_2}}\cos\left(\frac{b\lambda_k}{\sqrt{D_2}}\right)\sin\left(\frac{a\lambda_k}{\sqrt{D_1}}\right) + \frac{a}{2\lambda_k\sqrt{D_1}}\sin\left(\frac{b\lambda_k}{\sqrt{D_2}}\right)\cos\left(\frac{a\lambda_k}{\sqrt{D_1}}\right)\right]$$
$$+\sqrt{\frac{D_2}{D_1}}\left[\frac{a}{2\lambda_k\sqrt{D_1}}\cos\left(\frac{b\lambda_k}{\sqrt{D_2}}\right)\sin\left(\frac{a\lambda_k}{\sqrt{D_1}}\right) + \frac{b}{2\lambda_k\sqrt{D_2}}\sin\left(\frac{b\lambda_k}{\sqrt{D_2}}\right)\cos\left(\frac{a\lambda_k}{\sqrt{D_1}}\right)\right].$$

A.2 Removable singularity at $s = 0$

Recall

$$\bar{C}_2(x,s) = \frac{C_{1,0}}{s}\frac{F_2(x,s)}{\Delta(s)}, \qquad F_2(x,s) := \sinh\Big((b-x)\sqrt{\tfrac{s}{D_2}}\Big)\sinh\Big(a\sqrt{\tfrac{s}{D_1}}\Big).$$

Although $\bar{C}_2$ contains an explicit factor $1/s$, the point $s = 0$ is not a pole: the singularity is removable.

As $z \to 0$ we have the Taylor expansion $\sinh z = z + \mathcal{O}(z^3)$. With

$$A(s) := (b-x)\sqrt{\tfrac{s}{D_2}}, \qquad B(s) := a\sqrt{\tfrac{s}{D_1}},$$

it follows that, as $s \to 0$,

$$F_2(x,s) = \sinh(A(s))\sinh(B(s)) = \big(A(s) + \mathcal{O}(A(s)^3)\big)\big(B(s) + \mathcal{O}(B(s)^3)\big) = A(s)B(s) + \mathcal{O}(s^2).$$

Since $A(s)B(s) = a(b-x)\frac{s}{\sqrt{D_1 D_2}}$, we obtain

$$F_2(x,s) = \frac{a(b-x)}{\sqrt{D_1 D_2}}\, s + \mathcal{O}(s^2), \qquad s \to 0.$$

Moreover, $\Delta(0) = \sqrt{\frac{D_2}{D_1}} \neq 0$, because $\sinh(0) = 0$ and $\cosh(0) = 1$. Therefore,

$$\bar{C}_2(x,s) = \frac{C_{1,0}}{s}\frac{F_2(x,s)}{\Delta(s)} = C_{1,0}\,\frac{\frac{a(b-x)}{\sqrt{D_1 D_2}} + \mathcal{O}(s)}{\Delta(0) + \mathcal{O}(s)},$$

is bounded as $s \to 0$ and admits a finite limit. Hence $s = 0$ contributes no residue in the contour inversion.

B Unified Transform Method Proofs and Derivations

In this appendix we derive the global relations (9.GR: p)–(9.GR: q) from the transformed PDEs by integrating by parts twice.

B.1 Derivation for p

Recall that after applying the respective Fourier transform to (8.PDE1), we obtain

$$0 = \partial_t \hat{p}(\lambda, t) - D_1 \int_0^a e^{-i\lambda x} p_{xx}(x,t)\, dx.$$

Integration by parts twice gives:

$$\begin{aligned} 0 &= \partial_t \hat{p}(\lambda;t) - D_1 \left\{ \left[e^{-i\lambda x} p_x(x,t) + i\lambda e^{-i\lambda x} p(x,t) \right]_{x=0}^{x=a} - \lambda^2 \int_0^a e^{-i\lambda x} p(x,t) dx \right\} \\ &= (\partial_t + \lambda^2 D_1)\hat{p}(\lambda;t) - D_1 \left[\cancel{e^{-i\lambda a} p_x(a,t)} + i\lambda e^{-i\lambda a} p(a,t) - p_x(0,t) - i\lambda p(0,t) \right] \\ &= (\partial_t + \lambda^2 D_1)\hat{p}(\lambda;t) - D_1 \left[i\lambda e^{-i\lambda a} p(a,t) - p_x(0,t) - i\lambda p(0,t) \right]. \end{aligned}$$

Multiplying by $e^{D_1\lambda^2 t}$ and integrating from 0 to t gives the global relation

$$\hat{p}(\lambda;t) e^{D_1\lambda^2 t} = \hat{p}(\lambda,0) + D_1 \int_0^t e^{D_1\lambda^2 s} \left[i\lambda e^{-i\lambda a} p(a,s) - p_x(0,s) - i\lambda p(0,s) \right] ds.$$

Finally, since $p(x,0) = C_{1,0}$, we have

$$\hat{p}(\lambda,0) = \int_0^a e^{-i\lambda x} C_{1,0}\, dx = \frac{C_{1,0}}{i\lambda}\left(1 - e^{-i\lambda a}\right) =: \hat{P}(\lambda).$$

B.2 Derivation for q

Similarly, after applying the respective Fourier Transform to (8.PDE2), we obtain

$$0 = \partial_t \hat{q}(\lambda, t) - D_2 \int_0^b e^{-i\lambda x} q_{xx}(x,t)\, dx.$$

Integrating by parts twice as above gives

$$\int_0^b e^{-i\lambda x} q_{xx}(x,t)\, dx = e^{-i\lambda b} q_x(b,t) - q_x(0,t) + i\lambda\left(e^{-i\lambda b} q(b,t) - q(0,t)\right) - \lambda^2 \hat{q}(\lambda,t).$$

Hence

$$(\partial_t + D_2\lambda^2)\hat{q}(\lambda,t) = D_2\Big(e^{-i\lambda b} q_x(b,t) + i\lambda e^{-i\lambda b} q(b,t) - q_x(0,t) - i\lambda q(0,t)\Big).$$

Using the boundary condition $q(b,t) = 0$, we obtain

$$(\partial_t + D_2\lambda^2)\hat{q}(\lambda,t) = D_2\Big(e^{-i\lambda b} q_x(b,t) - q_x(0,t) - i\lambda q(0,t)\Big). \tag{21}$$

Multiplying (21) by $e^{D_2\lambda^2 t}$ and integrating from 0 to t gives

$$\hat{q}(\lambda,t) e^{D_2\lambda^2 t} = \hat{q}(\lambda,0) + D_2 \int_0^t e^{D_2\lambda^2 s}\Big(e^{-i\lambda b} q_x(b,s) - q_x(0,s) - i\lambda q(0,s)\Big)\, ds,$$

which is (9.GR: q). Since $q(x,0) = 0$, we have

$$\hat{q}(\lambda,0) = \int_0^b e^{-i\lambda x}\, 0\, dx = 0.$$

B.3 Replacing t by T in the spectral boundary values

In the derivation of the preliminary integral representations (10.P.1)–(10.P.2), the transforms $\hat{p}(\lambda;t)$ and $\hat{q}(\lambda;t)$ were expressed in terms of the spectral boundary values $f_j^\flat(\lambda;t)$, $g_j^\flat(\lambda;t)$ and $f_j^\#(\lambda;t)$, $g_j^\#(\lambda;t)$ and were defined with upper limit t. We now show that, in the contour integrals over $\partial\mathcal{D}^\pm$, we can replace this upper limit by any final time $T \geq t$ without changing the value of $p(x,t)$ or $q(x,t)$.

Lemma 0.2. Let $T \geq t \geq 0$. For all $x \in (0,a)$,

$$0 = \int_{\partial\mathcal{D}^+} e^{\,i\lambda x - D_1\lambda^2 t}\Big(\big[f_1^\flat(\lambda;T) - f_1^\flat(\lambda;t)\big] + i\lambda\,\big[f_0^\flat(\lambda;T) - f_0^\flat(\lambda;t)\big]\Big)\,d\lambda, \tag{22}$$

and for all $x \in (0,a)$,

$$0 = \int_{\partial\mathcal{D}^-} e^{\,i\lambda(x-a) - D_1\lambda^2 t}\Big(i\lambda\,\big[g_0^\flat(\lambda;T) - g_0^\flat(\lambda;t)\big]\Big)\,d\lambda. \tag{23}$$

Likewise, for all $x \in (0,b)$,

$$0 = \int_{\partial\mathcal{D}^+} e^{\,i\lambda x - D_2\lambda^2 t}\Big(\big[f_1^\#(\lambda;T) - f_1^\#(\lambda;t)\big] + i\lambda\,\big[f_0^\#(\lambda;T) - f_0^\#(\lambda;t)\big]\Big)\,d\lambda, \tag{24}$$

and for all $x \in (0,b)$,

$$0 = \int_{\partial\mathcal{D}^-} e^{\,i\lambda(x-b) - D_2\lambda^2 t}\Big(\big[g_1^\#(\lambda;T) - g_1^\#(\lambda;t)\big]\Big)\,d\lambda. \tag{25}$$

Proof. We prove the $f_0^\flat$ part of (22); the $f_1^\flat$ part is almost identical, with p replaced by p_x. The remaining claims (23)–(25) follow by the same argument, with the appropriate boundary traces, and (for the $\partial\mathcal{D}^-$ integrals) using that $\Im(\lambda) \leq 0$ on $\partial\mathcal{D}^-$ and $x-a<0$, $x-b<0$.

Since $s \mapsto p(0,s)$ is defined on the finite interval $[0,T]$, the map

$$\lambda \mapsto \int_0^T e^{D_1\lambda^2 s}\,p(0,s)\,ds,$$

is an entire function of λ. Therefore,

$$i\lambda\,e^{-D_1\lambda^2 t}\,\big[f_0^\flat(\lambda;T) - f_0^\flat(\lambda;t)\big] = i\lambda\int_t^T e^{D_1\lambda^2(s-t)}\,p(0,s)\,ds,$$

is entire.

Integrating by parts in s (and assuming $\lambda \in \overline{\mathcal{D}^+}$ and $T \geq t \geq 0$) gives

$$\begin{aligned} i\lambda\int_t^T e^{D_1\lambda^2(s-t)}\,p(0,s)\,ds &= i\lambda\left[\frac{e^{D_1\lambda^2(s-t)}}{D_1\lambda^2}\,p(0,s)\right]_{s=t}^{s=T} - i\lambda\int_t^T \frac{e^{D_1\lambda^2(s-t)}}{D_1\lambda^2}\,p_t(0,s)\,ds \\ &= \frac{i}{D_1\lambda}\left(e^{D_1\lambda^2(T-t)}\,p(0,T) - p(0,t) - \int_t^T e^{D_1\lambda^2(s-t)}\,p_t(0,s)\,ds\right). \end{aligned}$$

Hence

$$\left|i\lambda\,e^{-D_1\lambda^2 t}\,\big[f_0^\flat(\lambda;T) - f_0^\flat(\lambda;t)\big]\right| \leq \frac{1}{D_1|\lambda|}\left(\left|e^{D_1\lambda^2(T-t)}p(0,T)\right| + |p(0,t)| + \int_t^T \left|e^{D_1\lambda^2(s-t)}p_t(0,s)\right|\,ds\right).$$

For $\lambda \in \overline{\mathcal{D}^+}$ we have $\Re(D_1\lambda^2) \leq 0$, so

$$\left|e^{D_1\lambda^2(T-t)}\right| \leq 1, \qquad \left|e^{D_1\lambda^2(s-t)}\right| \leq 1 \quad (t \leq s \leq T).$$

Therefore,

$$\left|i\lambda\, e^{-D_1\lambda^2 t}\left[f_0^\flat(\lambda;T)-f_0^\flat(\lambda;t)\right]\right| \le \frac{1}{D_1|\lambda|}\left(|p(0,T)|+|p(0,t)|+\int_t^T |p_t(0,s)|\,ds\right),$$

so

$$i\lambda\, e^{-D_1\lambda^2 t}\left[f_0^\flat(\lambda;T)-f_0^\flat(\lambda;t)\right] = O(|\lambda|^{-1}), \qquad |\lambda|\to\infty \text{ within } \overline{\mathcal{D}^+},$$

uniformly in $\arg(\lambda)$.

Finally, for $x>0$ and λ in the upper half-plane, $|e^{i\lambda x}| = e^{-x\Im(\lambda)} \le 1$. Thus the integrand in (22) is $O(|\lambda|^{-1})$ on large arcs closing $\partial\mathcal{D}^+$, and since it is analytic in $\mathcal{D}^+$, Jordan's lemma (together with Cauchy's theorem) implies that the contour integral in (22) vanishes. This proves the $f_0^\flat$ contribution, and the other parts follow as noted above. □

By Lemma 0.2, the contour representations are unchanged if we replace the time-t spectral boundary values by their time-T counterparts. In particular, within the contour integrals we may use the shorthand

$$f_j^\flat(\lambda) := f_j^\flat(\lambda;T), \quad g_j^\flat(\lambda) := g_j^\flat(\lambda;T), \quad f_j^\#(\lambda) := f_j^\#(\lambda;T), \quad g_j^\#(\lambda) := g_j^\#(\lambda;T),$$

without changing $p(x,t)$ or $q(x,t)$.

Although the resulting "T-version" of the representation appears to involve boundary data for future times $s\in(t,T)$, Lemma 0.2 shows that these contributions integrate to zero, so there is no dependence of the solution on the future boundary values.

B.4 Proof of Lemma 0.1

We will just prove the f_0 part of (L0.1a); the f_1 part is almost identical. After the change of variables $\lambda\mapsto-\lambda$, the g_0 part (L0.1b) is also very similar.

As shown in standard Fourier analysis, the exponential Fourier transform of a function defined on a finite interval is an entire function. Here $f_0^\flat(\lambda;t)$ can be viewed as the exponential Fourier transform of $s\mapsto p(0,s)$ on $[0,t]$, evaluated at the complex frequency $iD_1\lambda^2$. Therefore,

$$i\lambda\, e^{-D_1\lambda^2 t}\, f_0^\flat(\lambda;t),$$

is an entire function of λ.

Integrating by parts once in the definition, and assuming $\lambda\in\overline{\mathcal{E}^+}$ and $t\ge 0$,

$$\begin{aligned} i\lambda\, e^{-D_1\lambda^2 t}\, f_0^\flat(\lambda;t) &= i\lambda\int_0^t e^{D_1\lambda^2(s-t)}\,p(0,s)\,ds \\ &= i\lambda\left[\frac{e^{D_1\lambda^2(s-t)}}{D_1\lambda^2}\,p(0,s)\right]_{s=0}^{s=t} - i\lambda\int_0^t \frac{e^{D_1\lambda^2(s-t)}}{D_1\lambda^2}\,p_t(0,s)\,ds \\ &= \frac{i}{D_1\lambda}\left(p(0,t)-e^{-D_1\lambda^2 t}p(0,0)-\int_0^t e^{D_1\lambda^2(s-t)}\,p_t(0,s)\,ds\right). \end{aligned}$$

Hence

$$\left|i\lambda\, e^{-D_1\lambda^2 t}\, f_0^\flat(\lambda;t)\right| \le \frac{1}{D_1|\lambda|}\left(|p(0,t)| + \left|e^{-D_1\lambda^2 t}p(0,0)\right| + \int_0^t \left|e^{D_1\lambda^2(s-t)}p_t(0,s)\right| ds\right).$$

Now for $\lambda \in \overline{\mathcal{E}^+}$ we have $\Re(D_1\lambda^2) \ge 0$, so

$$\left|e^{-D_1\lambda^2 t}\right| \le 1, \qquad \left|e^{D_1\lambda^2(s-t)}\right| = e^{\Re(D_1\lambda^2)(s-t)} \le 1 \quad (0 \le s \le t).$$

Therefore,

$$\left|i\lambda\, e^{-D_1\lambda^2 t}\, f_0^\flat(\lambda;t)\right| \le \frac{1}{D_1|\lambda|}\left(|p(0,t)| + |p(0,0)| + \int_0^t |p_t(0,s)|\, ds\right),$$

so

$$i\lambda\, e^{-D_1\lambda^2 t}\, f_0^\flat(\lambda;t) = O(|\lambda|^{-1}), \qquad |\lambda| \to \infty \text{ within } \overline{\mathcal{E}^+},$$

uniformly in $\arg(\lambda)$.

Multiplying by $e^{i\lambda x}$ does not affect the estimate on the closing arcs in $\mathbb{C}^+$, since $|e^{i\lambda x}| = e^{-x\Im(\lambda)} \le 1$ for $x > 0$ and $\Im(\lambda) \ge 0$. Thus the f_0 contribution in (L0.1a) has integrand $O(|\lambda|^{-1})$ on large arcs in $\overline{\mathcal{E}^+}$. By Jordan's lemma (with $x > 0$) and Cauchy's theorem, its contour integral over $\partial\mathcal{E}^+$ vanishes.

The f_1 part is identical, with p replaced by p_x. For (L0.1b), write $g_0^\flat(\lambda;t) = \int_0^t e^{D_1\lambda^2 s}p(a,s)\, ds$ and apply the same computation on $\overline{\mathcal{E}^-}$, noting that $x - a < 0$ and $|e^{i\lambda(x-a)}| \le 1$ for $\Im(\lambda) \le 0$.

B.5 Solution of the spectral system

For compactness set

$$\theta_1 := \frac{a\lambda}{\sqrt{D_1}}, \qquad \theta_2 := \frac{b\lambda}{\sqrt{D_2}},$$

and define the even/odd combinations

$$\hat{p}_\pm(\lambda) := \hat{p}\left(\frac{\lambda}{\sqrt{D_1}};T\right) \pm \hat{p}\left(-\frac{\lambda}{\sqrt{D_1}};T\right), \quad \hat{P}_\pm(\lambda) := \hat{P}\left(\frac{\lambda}{\sqrt{D_1}}\right) \pm \hat{P}\left(-\frac{\lambda}{\sqrt{D_1}}\right),$$
$$\hat{q}_\pm(\lambda) := \hat{q}\left(\frac{\lambda}{\sqrt{D_2}};T\right) \pm \hat{q}\left(-\frac{\lambda}{\sqrt{D_2}};T\right).$$

Algebraic reduction

Starting from (15)–(18), adding and subtracting (15) and (16) gives

$$2\sqrt{D_1}\,\lambda\sin(\theta_1)\, G_0^\flat(\lambda) + 2D_2 F_1^\#(\lambda) = e^{\lambda^2 T}\hat{p}_+(\lambda) - \hat{P}_+(\lambda), \tag{26}$$
$$2i\sqrt{D_1}\,\lambda\cos(\theta_1)\, G_0^\flat(\lambda) - 2i\sqrt{D_1}\,k_m\lambda\, F_0^\#(\lambda) = e^{\lambda^2 T}\hat{p}_-(\lambda) - \hat{P}_-(\lambda). \tag{27}$$

Similarly, adding and subtracting (17) and (18) yields

$$F_1^\#(\lambda) = \cos(\theta_2)\, G_1^\#(\lambda) - \frac{e^{\lambda^2 T}}{2D_2}\,\hat{q}_+(\lambda), \tag{28}$$
$$2i\lambda\, F_0^\#(\lambda) = -2i\sqrt{D_2}\sin(\theta_2)\, G_1^\#(\lambda) - \frac{e^{\lambda^2 T}}{\sqrt{D_2}}\,\hat{q}_-(\lambda). \tag{29}$$

Substituting (28) into (26) and dividing by 2 gives

$$\sqrt{D_1}\,\lambda\sin(\theta_1)\,G_0^{\flat}(\lambda)+D_2\cos(\theta_2)\,G_1^{\#}(\lambda)=R_1(\lambda), \tag{30}$$

where

$$R_1(\lambda):=\frac{e^{\lambda^2T}}{2}\big(\hat{p}_+(\lambda)+\hat{q}_+(\lambda)\big)-\frac{1}{2}\hat{P}_+(\lambda).$$

Next, using (29) inside (27) and dividing by $2i\sqrt{D_1}$ gives

$$\lambda\cos(\theta_1)\,G_0^{\flat}(\lambda)+k_m\sqrt{D_2}\sin(\theta_2)\,G_1^{\#}(\lambda)=R_2(\lambda), \tag{31}$$

where

$$R_2(\lambda):=\frac{1}{2i\sqrt{D_1}}\Big(e^{\lambda^2T}\Big[\hat{p}_-(\lambda)-\frac{k_m\sqrt{D_1}}{\sqrt{D_2}}\hat{q}_-(\lambda)\Big]-\hat{P}_-(\lambda)\Big).$$

Equations (30)–(31) may be written as

$$M(\lambda)\begin{pmatrix}G_0^{\flat}(\lambda)\\ G_1^{\#}(\lambda)\end{pmatrix}=\begin{pmatrix}R_1(\lambda)\\ R_2(\lambda)\end{pmatrix},\qquad M(\lambda):=\begin{pmatrix}\sqrt{D_1}\lambda\sin(\theta_1) & D_2\cos(\theta_2)\\ \lambda\cos(\theta_1) & k_m\sqrt{D_2}\sin(\theta_2)\end{pmatrix}. \tag{32}$$

A short computation gives

$$\Delta(\lambda):=\det M(\lambda)=\lambda\Big(k_m\sqrt{D_1D_2}\,\sin(\theta_1)\sin(\theta_2)-D_2\cos(\theta_1)\cos(\theta_2)\Big), \tag{33}$$

$$\Delta_{\text{core}}(\lambda):=\frac{\Delta(\lambda)}{\lambda}=k_m\sqrt{D_1D_2}\,\sin(\theta_1)\sin(\theta_2)-D_2\cos(\theta_1)\cos(\theta_2). \tag{34}$$

By Cramer's rule,

$$G_0^{\flat}(\lambda)=\frac{k_m\sqrt{D_2}\sin(\theta_2)\,R_1(\lambda)-D_2\cos(\theta_2)\,R_2(\lambda)}{\Delta(\lambda)}, \tag{35}$$

$$G_1^{\#}(\lambda)=\frac{\lambda\big(\sqrt{D_1}\sin(\theta_1)\,R_2(\lambda)-\cos(\theta_1)\,R_1(\lambda)\big)}{\Delta(\lambda)}=\frac{\sqrt{D_1}\sin(\theta_1)\,R_2(\lambda)-\cos(\theta_1)\,R_1(\lambda)}{\Delta_{\text{core}}(\lambda)}. \tag{36}$$

Then (28)–(29) give

$$F_1^{\#}(\lambda)=\cos(\theta_2)\,G_1^{\#}(\lambda)-\frac{e^{\lambda^2T}}{2D_2}\,\hat{q}_+(\lambda), \tag{37}$$

$$2i\lambda F_0^{\#}(\lambda)=-2i\sqrt{D_2}\sin(\theta_2)\,G_1^{\#}(\lambda)-\frac{e^{\lambda^2T}}{\sqrt{D_2}}\,\hat{q}_-(\lambda). \tag{38}$$

Vanishing of the T-dependent contributions

The quantities $R_1(\lambda)$ and $R_2(\lambda)$ contain terms proportional to $e^{\lambda^2T}\hat{p}_\pm(\lambda)$ and $e^{\lambda^2T}\hat{q}_\pm(\lambda)$. When $T>t$ these parts do not contribute after substitution into the contour integrals for $p(x,t)$ and $q(x,t)$.

Indeed, $\hat{p}(\cdot;T)$ and $\hat{q}(\cdot;T)$ are entire functions of the spectral parameter (exponential Fourier transforms on finite intervals), hence so are $\hat{p}_\pm,\hat{q}_\pm$. Within the contour integrals one encounters the factor

$$e^{-D_j\lambda^2t}\,e^{\lambda^2T}=e^{D_j\lambda^2(T-t)}.$$

On $\partial\mathcal{D}^{\pm}$ we have $\Re(\lambda^2) < 0$, so for $T > t$ this factor decays exponentially as $|\lambda| \to \infty$. Since the remaining factors are analytic in the relevant domains, Jordan's lemma and Cauchy's theorem imply that the contour integrals of the T-dependent parts vanish. Consequently, *within the contour integrals* we may replace

$$R_1(\lambda) \mapsto -\frac{1}{2}\hat{P}_+(\lambda), \qquad R_2(\lambda) \mapsto -\frac{1}{2i\sqrt{D_1}}\hat{P}_-(\lambda), \tag{39}$$

and use (35)–(38) with these simplified right-hand sides.

For reference, define

$$\widetilde{R}_1(\lambda) := -\frac{1}{2}\hat{P}_+(\lambda), \qquad \widetilde{R}_2(\lambda) := -\frac{1}{2i\sqrt{D_1}}\hat{P}_-(\lambda),$$

and the corresponding spectral functions

$$\widetilde{G}_0^{\flat}(\lambda) := \frac{k_m\sqrt{D_2}\sin(\theta_2)\,\widetilde{R}_1(\lambda) - D_2\cos(\theta_2)\,\widetilde{R}_2(\lambda)}{\Delta(\lambda)},$$

$$\widetilde{G}_1^{\#}(\lambda) := \frac{\sqrt{D_1}\sin(\theta_1)\,\widetilde{R}_2(\lambda) - \cos(\theta_1)\,\widetilde{R}_1(\lambda)}{\Delta_{\text{core}}(\lambda)},$$

$$\widetilde{F}_1^{\#}(\lambda) := \cos(\theta_2)\,\widetilde{G}_1^{\#}(\lambda), \qquad 2i\lambda\widetilde{F}_0^{\#}(\lambda) := -2i\sqrt{D_2}\sin(\theta_2)\,\widetilde{G}_1^{\#}(\lambda).$$

By the vanishing argument above, the parts of $R_1(\lambda)$ and $R_2(\lambda)$ proportional to $e^{\lambda^2 T}\hat{p}_{\pm}(\lambda)$ and $e^{\lambda^2 T}\hat{q}_{\pm}(\lambda)$ do not contribute once substituted into the contour integrals for $p(x,t)$ and $q(x,t)$ (with $T > t$). Hence, we may replace our spectral functions $G_0^{\flat}, G_1^{\#}, F_0^{\#}, F_1^{\#}$ with $\widetilde{G}_0^{\flat}, \widetilde{G}_1^{\#}, \widetilde{F}_0^{\#}, \widetilde{F}_1^{\#}$ in the integrands.

Reproducibility note

Numerical evaluations of the Laplace-series representation (6)–(7) were performed by computing the first K positive roots $\{\lambda_k\}_{k=1}^{K}$ of (5) using bracketing and `fzero`, and then summing the truncated series with coefficients involving $\Delta'(-\lambda_k^2)$ (Appendix A.1).

For the UTM, p and q were evaluated from the contour representations (19)–(20) using the simplified spectral data $\widetilde{R}_1, \widetilde{R}_2$ (i.e. omitting the T-dependent contributions as justified in Appendix B.5). The real-line integral in p was truncated to $[-L_{\text{real}}, -\varepsilon] \cup [\varepsilon, L_{\text{real}}]$, and the contour integrals over $\partial\mathcal{D}^{\pm}$ were evaluated by quadrature along two rays $\lambda = r(-c \pm i)$ and $\lambda = r(c \pm i)$, $r \in [\varepsilon, R_{\max}]$, closed by a small circular connector arc of radius ε to avoid the pole at $\lambda = 0$. The truncation parameters L_{real} and $R_{\max}$ were chosen from the decay of $e^{-D_j\lambda^2 t}$ using a prescribed tolerance, and quadrature was performed with tight relative and absolute tolerances.

To preserve space within the appendix page limit, the full MATLAB implementation is omitted, but the formulas, contour parametrisations, and parameter values stated in the report are sufficient to reproduce all numerical results.

References

Fernandes, M, Simon, L & Loney, NW 2005, 'Mathematical modeling of transdermal drug-delivery systems: Analysis and applications', *Journal of Membrane Science*, vol. 256, pp. 184–192.

Prausnitz, MR & Langer, R 2008, 'Transdermal drug delivery', *Nature Biotechnology*, vol. 26, no. 11, pp. 1261–1268.

Sheils, NE 2017, 'Multilayer diffusion in a composite medium with imperfect contact', *Applied Mathematical Modelling*, vol. 46, pp. 450–464.

Rodrigo, MR & Worthy, AL 2016, 'Solution of multilayer diffusion problems via the Laplace transform', *Journal of Mathematical Analysis and Applications*, vol. 444, pp. 475–502.

Guy, RH & Hadgraft, J 1985, 'Transdermal drug delivery: a simplified pharmacokinetic approach', *International Journal of Pharmaceutics*, vol. 24, pp. 267–274.

Deconinck, B, Pelloni, B & Sheils, N 2014, 'Non-steady state heat conduction in composite walls', *Proceedings of the Royal Society A*, vol. 470, no. 2165, 20130605.

Deconinck, B, Trogdon, T & Vasan, V 2014, 'The Method of Fokas for Solving Linear Partial Differential Equations', *SIAM Review*, vol. 56, no. 1, pp. 159–186.